Radiation and Propagation
in the Context of HF Over-The-Horizon Radar

Yannick Béniguel

IEEA

Courbevoie, France

beniguel@ieea.fr

Muriel Darces, Marc Hélier, Nicolas Payet

UPMC Univ Paris 06, UR2, L2E, BC 252

F-75005 Paris, France

muriel.darces@upmc.fr

Abstract—**This paper addresses the issue of the propagation of electromagnetic waves radiated by HF antennas located in the vicinity of an infinite plane interface. This point is of major interest when dealing with over-the-horizon radar applications. Two numerical approaches aimed at the computation of the spatial electric field distribution radiated by typical HF antennas are described and compared.**

Index Terms— mixed potential equation; Sommerfeld integrals; near field to far field transformation; surface wave; sky wave;

I. INTRODUCTION

HF over-the-horizon radars are observation tools used for the surveillance of large maritime zones. They can detect targets beyond the line-of-sight. There are two modes of wave propagation defining the so-called "sky-wave" HF radars and the "surface-wave" HF radars. The sky-wave mode is associated to a propagation by ionospheric reflection and the surface-wave mode to a propagation at the air - ground interface. Whatever the type of HF radar, these two modes coexist. Both are drastically influenced by the environment of the transmitting antennas and particularly by the electromagnetic properties of the ground upon which they are located. In consequence, the knowledge of the antenna radiation is of major interest in order to estimate the efficiency of the device in relation to the dedicated wave mode.

As a characteristic example, the radiation of a vertical Hertzian dipole located on a half-space ground is studied. The distribution of the vertical component E_θ of the electric field radiated by a Hertzian dipole placed and on a dry ground ($\varepsilon_r = 15$, $\sigma = 0.05$ S.m^{-1}) is depicted, in Fig. 1, at two distances (1 km and 10 km) from the source. In that case, the working frequency is 3 MHz. The curves are compared with those corresponding to the perfect electric conductor (PEC) ground, considered as a reference, and independent of the distance. It appears that, in both cases, the surface wave is not negligible and vanishes at more or less large distance from the antenna, depending on the ground properties. In that sense, in HF band, it becomes impossible to define a unique far field pattern since it changes with the distance of observation.

Two numerical methods aimed at the computation of the electric field radiated by typical HF antennas in the far zone have been developed and implemented.
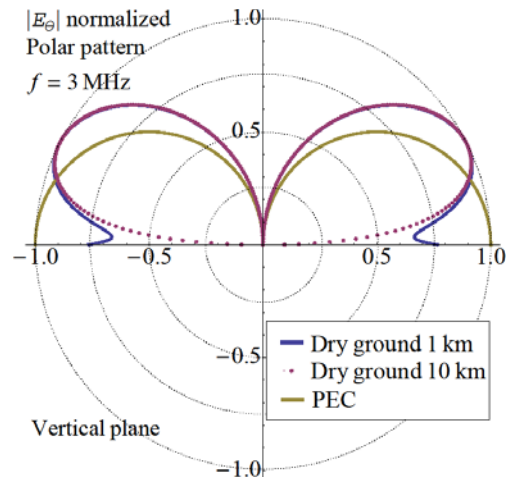

Figure 1. Radiation of a vertical Hertzian dipole located on a dry land- the surface wave cannot be neglected

The first part of this paper describes a method based on the resolution of the Mixed Potential Integral Equation (MPIE). The second part describes a method based on a near field to far field (NF/FF) transformation. The third one shows the comparison of these two approaches and concludes on their respective advantages.

II. MIXED POTENTIAL INTEGRAL EQUATION

The Electromagnetic Field Integral Equation (EFIE) technique is a very well suited technique for antenna analysis. It allows considering surfaces and wire elements, including dielectric parts as lenses or substrates. Using the method of moments, the analysis technique only considers interfaces between media. These interfaces are meshed into surface or wire elements which constitute the problem unknowns.

The HF antennas problem brings one additional complexity to the problem. Taking the infinite interface into account requires modifying the EFIE. The new equation, named Mixed Potential Integral Equation (MPIE) [1], includes additional terms allowing to meet the boundary conditions on the interface. In the case of a metallic structure, the MPIE equation can be written as :

$$\mathbf{E}^s = -j\,\omega\,\mathbf{A} - \nabla\Phi \qquad (1)$$

With for the vector potential

$$A = \int \overline{G}^A (r, r') . J_s (r') \, ds' \qquad (2)$$

$$G^A = G^A_{vv} + \hat{z} \hat{u} \, G^A_{zu} + \hat{z} \hat{z} \, G^A_{zz}$$

The normal to the interface is the z vector. In the above notation, $\hat{z} \hat{u}$ refers to the vertical (z) contribution of a dipole located in the horizontal (u) plane. The modified scalar potential and the relation between the potentials are the following :

$$\Phi = \int_S K_\Phi (r, r') \nabla'. J_s (r') \, ds'$$
$$- \int_C K_\Phi (r, r') J_s (r') . \hat{n} \, d\ell' \qquad (3)$$

$$\frac{j\omega}{k_i^2} \nabla . \overline{G}^A (r, r') = - \nabla' K_\Phi (r, r') \qquad (4)$$

All terms involved include the calculation of the Sommerfeld integrals. In this study these integrals are calculated using the complex image technique which allows separating the different contributions, in particular the one related to the surface wave [2].

The MPIE integral terms can be written in the general form as:

$$F(\rho) = \frac{1}{2\pi} \int_0^\infty f(k_\rho) J_n(k_\rho \rho) k_\rho \, dk_\rho \qquad (5)$$

with n equal 0 or 1. A special case of these integrals corresponds to the following, known as the Weyl identity:

$$G = \frac{\exp(-jkR)}{R} = \int_0^\infty \frac{\exp(-jk_z |z|)}{j k_z} J_0(k_\rho\rho) k_\rho dk_\rho \qquad (6)$$

In the classical derivation of the problem as introduced by Sommerfeld [3], double derivatives with respect to the radial and vertical distances are introduced. This creates a difficulty when trying to implement this in a classical EFIE code with rooftop basis functions (both on wires and on surfaces). The calculation can be performed alternatively in the spectral domain. Taking space derivative into account increases the Bessel function order in the above integral and can be addressed more easily.

Another benefit to perform the calculation in the spectral domain is the fact that it allows isolating the different contributions, then to subtract them from the integrand in order to get regular functions more suited to a numerical evaluation. There is one final additional benefit in this technique which consists in using the k_z complex integration plane instead of the k_ρ complex plane. In the k_z plane, a very simple linear integration contour can be defined making the calculation much easier to be carried out.

Each $F(\rho)$ integral is the sum of three contributions :

- A quasi - dynamic contribution which corresponds to the value of $f(k_\rho)$ when $k_\rho \rightarrow \infty$. This value is

subtracted from the integrand which is then equal to 0 for high k_ρ values. The removed part contribution is calculated analytically.
- A regular part approximated by a sum of exponential terms amenable to a sum of Weyl like identities with R_i as complex distances.
- A pole contribution with extraction of the singular part replaced by the sum of residues contribution.

This way to proceed is illustrated on figures 2 and 3. Figure 2 shows the regular part behavior of some of the terms and their approximation by a sum of complex exponential terms. All terms exhibit a very fast decay and can consequently be easily evaluated. Figure 3 shows the weight of the different contributions depending on the radial distance between the source and observation points. This is however strongly dependent on the medium electrical constants.
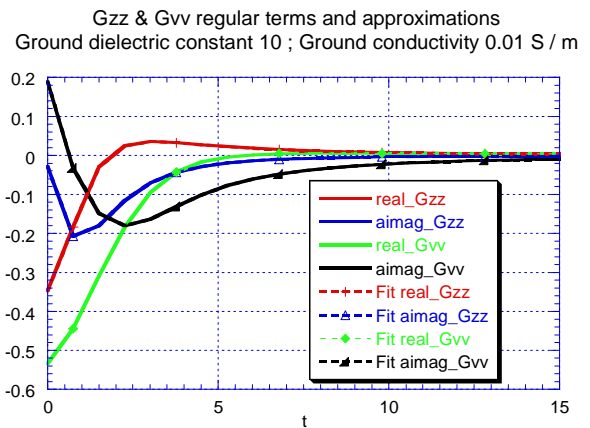

Figure 2 : Regular terms behaviour along the contour in the k_z complex plane and their approximation by a sum of complex exponential terms. Variable t is the coordinate along the integration contour
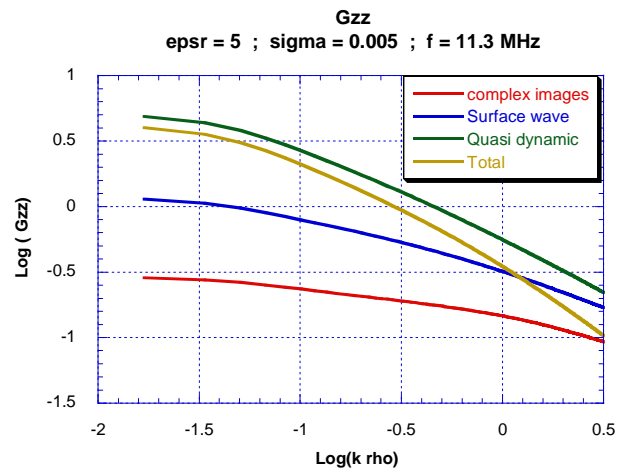

Figure 3 : the respective weight of the different contributions

The extraction of the quasi dynamic and of the poles contributions is still amenable in the case of an arbitrary number of layers with dipoles (either surface elements or wires) located in the different media.

III. NEAR FIELD TO FAR FIELD TRANSFORMATION

The second method is based on a source identification assuming that the antenna (or antenna network) under test (AUT) can be replaced by a set of equivalent dipoles radiating the same far field as the AUT [3]. This approach, based on the equivalence principle, has been already described by several authors [4, 5]. Nevertheless, the innovative point brought by this method is the use, as dipole's radiation function, of the analytic formulations developed by Norton and extended by Bannister [6] to the very near field zone. These formulations include the sky wave as well as the surface wave contributions of the electromagnetic field radiated by each elementary dipole.

Consider an AUT located at the plane horizontal interface between air and real ground. In a cylindrical coordinate system (ρ, φ, z), the components of the electromagnetic field are measured in the near-field zone (in order to measure the surface wave) on a virtual surface S_M surrounding the AUT. For convenience, we will first assume that S_M is a cylindrical surface, of radius r_{SM} and height h_{SM}, centered on the AUT (see Fig. 4). The surface S_M is meshed with a maximum spatial sampling step equal to $\lambda/2$, where λ is the wavelength. The number of measured points is N_M.
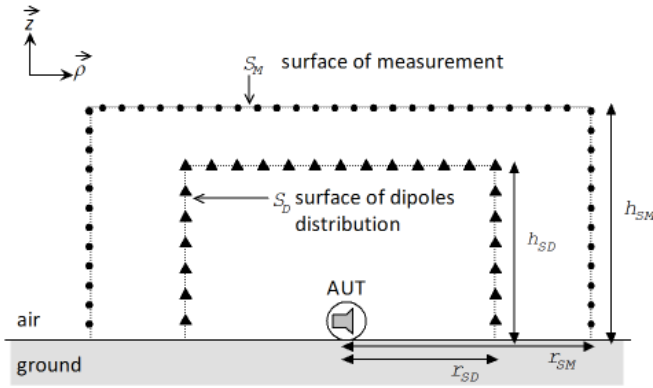

Figure 4.   Geometry corresponding to the method

Consider now a second virtual surface S_D, included inside the surface S_M. Also, for convenience, the surface S_D is supposed to be a cylinder of radius r_{SD} and height h_{SD}, centered on the AUT (see Fig. 4). It is also meshed with a maximum spatial sampling step equal to $\lambda/2$. The number of mesh points is N_D. At each point, three elementary electric dipoles are arranged in order to form an orthogonal basis aligned with the cylindrical basis vectors (see Fig. 5).

The method states that, at each point of the surface S_M, the electromagnetic field, is equal to the sum of all the contributions coming from each of the $3N_D$ dipoles spread on the surface S_D. This leads to the following matrix equations:

$$E_{SM} = D_E . P_{SD} \qquad (7)$$

$$H_{SM} = D_H . P_{SD} \qquad (8)$$

where E_{SM} and H_{SM} are respectively the electric and magnetic vectors of size $3N_M$, measured at each point on the surface S_M. D_E and D_H are respectively the electric and magnetic radiation matrices (issued from the Norton/Bannister formulations), of size $3N_M \times 3N_D$, concerning the $3N_D$ electric (horizontal and vertical) dipoles located at each point of the surface S_D. P_{SD} is the unknown vector, of size $3N_D$, containing the electric moments of the previous dipoles.
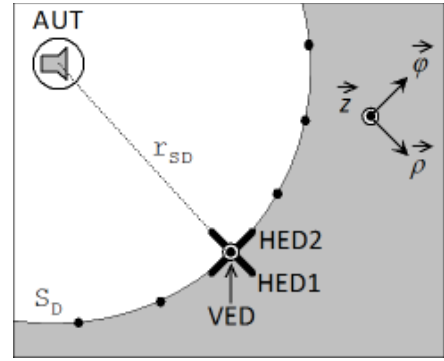

Figure 5.   Arrangement of two horizontal (HED1 and HED2) and one vertical (VED) electric dipoles at each sampling point of the surface S_D.

Equations (7) and (8) can be written in the following reduced form

$$(E\_H)_{SM} = D_{E\_H} . P_{SD} \qquad (9)$$

and solved by inversion of the matrix D_{E_H} in order to determine the vector P_{SD}.

The accuracy of the inversion is influenced by the number of dipoles contributing to the radiation. Particularly, it is necessary to unselect the dipoles which have a non-significant contribution to the total field. As a consequence, this inversion is carried out by applying a singular value decomposition (SVD) to the matrix D_{E_H} associated with a threshold power criterion. This criterion represents the total power radiated by the AUT, in the near-field, and is calculated from the measurement of the electromagnetic field on the surface S_M. Then the singular values matrix is scanned by decreasing order until the corresponding calculated power reaches this power criterion. Once the vector P_{SD} is determined, the electric far field can be easily computed from the direct linear system (9).

IV. ASSOCIATION OF THE METHODS AND RESULTS

The methods have been tested and combined in order to study two types of typical HF antennas.

The first example is a biconical HF antenna, depicted in figure 6, located on a dry ground ($\varepsilon_r = 13$ and $\sigma = 0.05$ S.m^{-1}), operating at a frequency of 10 MHz. Figure 7 shows the near field pattern, computed by the MPIE method, in a 200 m x 200 m vertical plane surface located at 30 m from the source in the horizontal direction. The sky-wave mode can be observed as well as the surface-wave mode that exhibits a peak value at the interface plane. Figure 8 depicts, in a vertical plane, the θ-component (magnitude and phase) of the electric field computed by the NF/FF transformation at an observation distance equal to 1 km. These far-field results are compared with the well-known code NEC/SOMNEC. The surface-wave is observable again for a value of the polar angle θ close to 90°, even at large distance from the source.
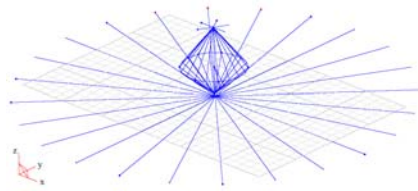
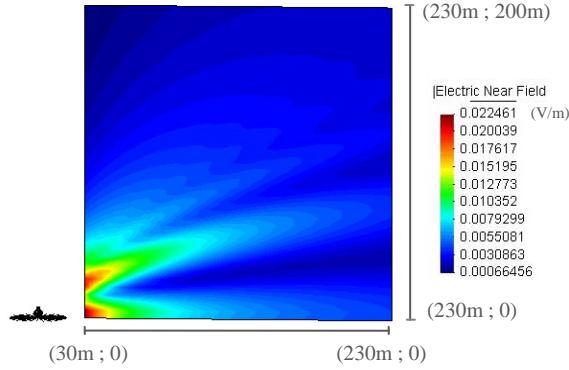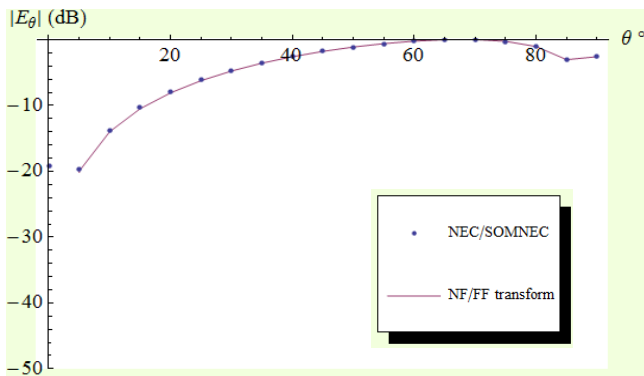Figure 6.   Antenna geometry: biconical antenna .
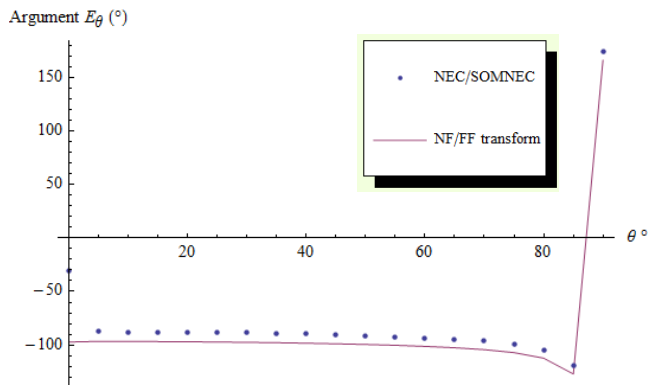

Figure 7.   Magnitude of the electric field radiated in the near zone by the biconical antenna over a dry ground – f=10 MHz

a. magnitude

b. phase

Figure 8.   Magnitude (a) and phase (b) of the θ-component of the electric field radiated by the biconical antenna at a distance R=1 km over a dry ground f=10 MHz

The second example is about a three vertical quarter-wavelength monopoles network, aligned along the *y* axis, as shown in figure 9, separated by a half-wavelength from each other, located on a sea water interface at 30 MHz operating frequency.
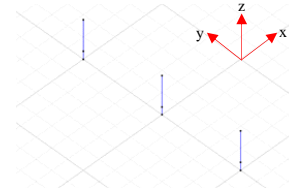

Figure 9.   Antenna geometry: monopole network .

Figures 10 and 11 show the near field pattern, computed by the MPIE method, on a 200 m x 200 m surface, horizontally located at 30 m from the source, in the φ=0° and φ=140° vertical planes, respectively.
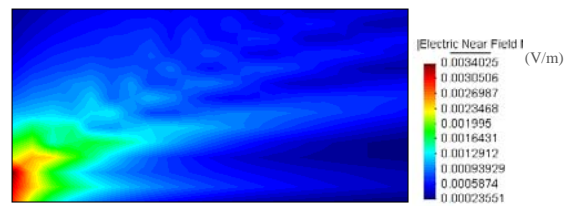

Figure 10. Magnitude of the electric field radiated in the near zone by the monopole network over a sea water ground – f=30 MHz – vertical plane φ=0°
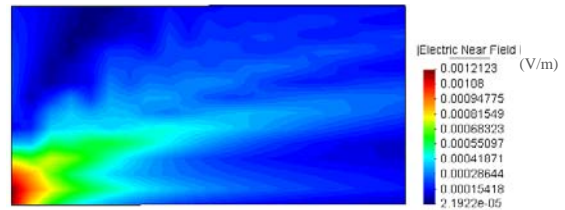

Figure 11. Magnitude of the electric field radiated in the near zone by the monopole network over a sea water ground - f=30 MHz -vertical plane φ=140°

This configuration allows highlighting the effect of a rotationally nonsymmetrical radiation with respect to the azimuth angle φ as well as a change of the ground electrical characteristics.

Figure 12 depicts, in the vertical plane φ=0°, the θ-component (magnitude and phase) of the electric field computed by the NF/FF transformation at an observation distance equal to 1 km. Figure 13 depicts, in the vertical plane φ=140°, the θ-component (magnitude and phase) of the electric field computed by the NF/FF transformation at an observation distance equal to 1 km.

The results obtained for the magnitude of the main component E_θ of the electric field in the far zone are in good agreement with the code NEC/SOMNEC, used as the reference one. Differences appear on the argument of the component. The method is more sensitive, from this point of view, to the high number of equivalent dipoles involving in the modeling of the AUT and combining each with the others.

Figure 12. Magnitude (a) and phase (b) of the θ-component of the electric field radiated by the monopole network at a distance R=1 km over a sea water ground f=10 MHz – vertical plane φ=0°

Figure 13. Magnitude (a) and phase (b) of the θ-component of the electric field radiated by the monopole network at a distance R=1 km over a sea water ground f=10 MHz – vertical plane φ=140°

V. CONCLUSION

The analysis of antennas located in the vicinity of a lossy infinite interface has been presented. Two complementary techniques were developed allowing to consider a large number of complex environments.

A numerical technique based on a solution of the electric field integral equations was developed. The algorithm allows considering infinite lossy interfaces as is the case for HF antennas and to separate the different contributions. It provides in particular the near field radiated by the antenna which was shown to exhibit the two contributions related to the surface wave and to the sky wave.

The near field to far field transformation is specific in that case due to the presence of the interface. A dedicated algorithm was developed. It can take as an input either the theoretical results or the measurements. It also provides a hint for the measurement campaign, if any, to locate and / or minimize the number of measurements points.

These two tools are combined for an accurate characterization of the antenna near field and far field distributions of particular interest for radar applications and complex environments such as the coastal region and ground – sea propagation for maritime surveillance purposes.

REFERENCES

[1] Michalski K., D. Zheng, "Electromagnetic Scattering and Radiation by Surfaces of Arbitrary Shape in Layered Media, Part I: Theory", IEEE AP, Vol 38, N° 3, 1990

[2] Béniguel, Y., "Antenna radiation in the presence of an infinite interface", *Antenna Technology and Applied Electromagnetics (ANTEM), 2012 15th International Symposium on* ,25-28 june 2012

[3] Payet, N.; Darces, M.; Montmagnon, J.-L.; Hélier, M.; Jangal, F.; , "Near field to far field transformation by using equivalent sources in HF band," *Antenna Technology and Applied Electromagnetics (ANTEM), 2012 15th International Symposium on* , vol., no., pp.1-4, 25-28 June 2012. doi: 10.1109/ANTEM.2012.6262318

[4] Regue, J.-R.; Ribo, M.; Gomila, J.; Perez, A.; Martin, A.; , "Modeling of radiating equipment by distributed dipoles using metaheuristic methods," Electromagnetic Compatibility, 2005. EMC 2005. 2005 International Symposium on, vol.2, no., pp.596-601, 12-12 Aug. 2005.

[5] Fan, F.; Schlagenhaufer, F.; , "Source identification and correlation between near field-far field tolerances when applying a genetic algorithm," Electromagnetic Compatibility - EMC Europe, 2008 International Symposium on, vol., no., pp.1-6, 8-12 Sept. 2008.

[6] Bannister, P.; , "The quasi-near fields of dipole antennas," *Antennas and Propagation, IEEE Transactions on* , vol.15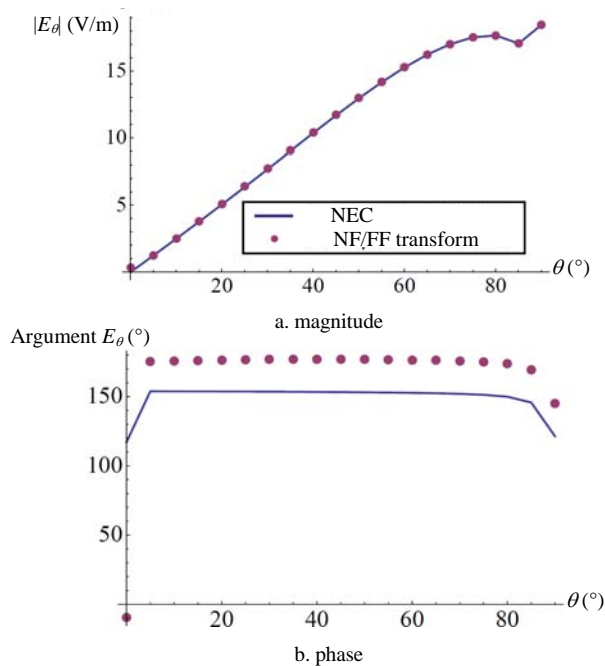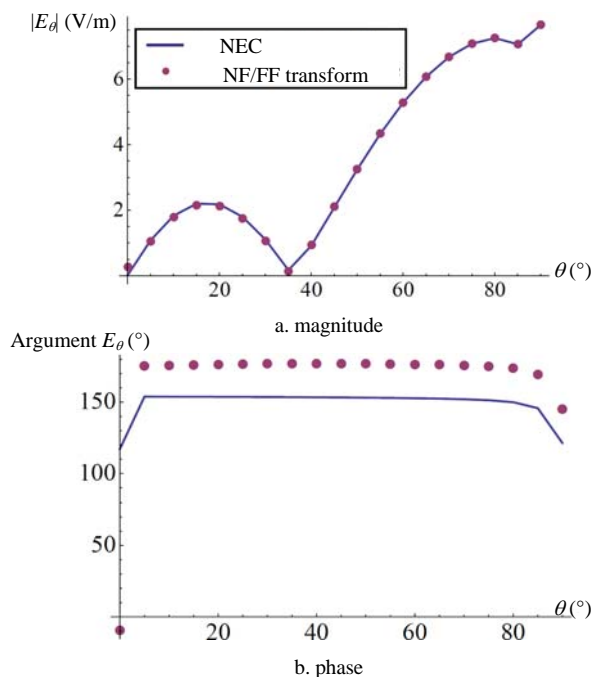, no.5, pp. 618- 626, Sept 1967.